Journal of Alloys and Compounds 509 (2011) 6806–6811

Contents lists available at ScienceDirect

Journal of Alloys and Compounds

journal homepage: www.elsevier.com/locate/jallcom

Oxidation of etched Zn foil for the formation of ZnO nanostructure

W.K. Tan [a], K. Abdul Razak [a], K. Ibrahim [b,**], Zainovia Lockman [a,*]

[a] Green Electronics Nanomaterials Group, School of Materials and Mineral Resources, Universiti Sains Malaysia, Engineering Campus, 14300 Nibong Tebal, Pulau Pinang, Malaysia
[b] Nano Optoelectronic Research Laboratory, School of Physics, Universiti Sains Malaysia, 11800 Pulau Pinang, Malaysia

ARTICLE INFO

Article history:
Received 25 November 2010
Accepted 9 March 2011
Available online 4 April 2011

Keywords:
Oxide materials
Nanostructured materials
Oxidation

ABSTRACT

Oxidation of Zn foil at temperatures of 100–400 °C was carried out in air to produce ZnO with various nanostructures. The final morphology of the oxidised Zn foil is largely dependent on the oxidation temperatures. At less than 300 °C, spherical oxide grains are seen. At 400 °C, 50 nm thick, porous nanosheets were formed after 30 min of oxidation. In portions of the samples, nanorods can be seen with diameters <10 nm and lengths reaching 1 μm. The nanosheets were formed in accordance to a vapour–solid mechanism whereas the nanorods were formed by diffusion of Zn through a certain path leading to the rod structure. At 450 °C, the nanorods became much more uniform. Oxidation at 500 °C resulted in ZnO nanorods. The rods are also blunt with smaller rods seen to branch out from the main rod. The luminescence properties of the ZnO were investigated as a function of the morphology of the oxide. Both green and blue emissions are seen for the samples with nanosheets whereas the nanorods ZnO has mostly green emission.

1. Introduction

ZnO is a wide band gap semiconductor (3.37 eV) with large exciton binding energy (60 meV) [1]. It is an exceptionally versatile compound for applications in electronics and optoelectronics, especially as material for: data storage, sensors, emission devices and photocatalyst [2,3]. For these applications, nanostructured ZnO is preferred as it has higher surface area and much better electronic transport properties. Works on the formation of ZnO nanostructures have been targeted at the development of synthesis methods that can give a good control over the dimensions of the nanostructure produced. These methods include: physical vapour deposition and chemical methods [1,4]. Despite the formation of interesting ZnO nanostructure by both methods, vapour deposition methods have always seen as more complicated as these methods would require rather complex equipment. On the other hand, chemical based methods are seen as contenders in the formation of well control ZnO nanostructures. In an effort to produce the nanostructures with an even simpler method, oxidation is proposed as an alternative technique [5–11]. By the use of oxidation, the formation of ZnO covering a large area at a short time will be possible. In the formation of nanostructured ZnO, oxidation works have been targeted not only on the oxidation of Zn foil but also the oxidation of thin Zn film on substrates like glass [5,6], silica and sapphire [7]. Oxidation of powdered Zn particles under various oxidation atmospheres have also been explored by many authors [8–11]. In this work, oxidation of etched Zn foil was performed at wide temperature range to explore on the morphologies evolution as a function of oxidation times and temperatures. During oxidation, it is speculated that at ultra-low temperature, the oxide will be flat and upon the increase of the temperature nanorods may form. Nonetheless, it was observed that in a low temperature regime, porous nanosheets were formed; and as the temperature increases, nanorods emerged and as the oxidation temperature was further increased, blunt branched nanorods were observed. Among these structures produced, perhaps the porous nanosheets structure is the most interesting as the porous structure can greatly enhance the active surface area available for either catalytic or sensing applications.

2. Experimental

99.95% pure Zn foils were oxidised in air to study the effect of oxidation temperatures and time on oxide structure formation on the Zn surface. The zinc foils that were used consisted of 99.95% purity. The Zn foils were cut into the desired dimensions (2 cm × 2 cm) and then ground using SiC paper with ascending grit. After grinding, the Zn foils are polished using alumina powder at 1 μm and 0.05 μm, respectively until a mirror-like surface was obtained. The Zn foils were cleaned an ultrasonic acetone bath for 15 min before being chemically etched using 5% of HCl in ethanol for 3 min. The Zn foils were then oxidised at two different times of 30 min and 1 h at temperatures of 100–500 °C in air. The Zn foil was placed in a pre-heated furnace at the desired oxidation temperature and was then quenched in air to room temperature after the oxidation period was achieved. The surface morphologies of oxidised Zn foils were viewed under a ZEISS SUPRA 35VP Field Emission Scanning Electron Microscope (FESEM). X-ray diffraction (XRD) Siemens D5000 was used for

* Corresponding author.
** Co-corresponding author.
E-mail addresses: Khairunisak@eng.usm.my (K. Ibrahim), zainovia@eng.usm.my (Z. Lockman).

0925-8388/$ – see front matter © 2011 Elsevier B.V. All rights reserved.
doi:10.1016/j.jallcom.2011.03.055

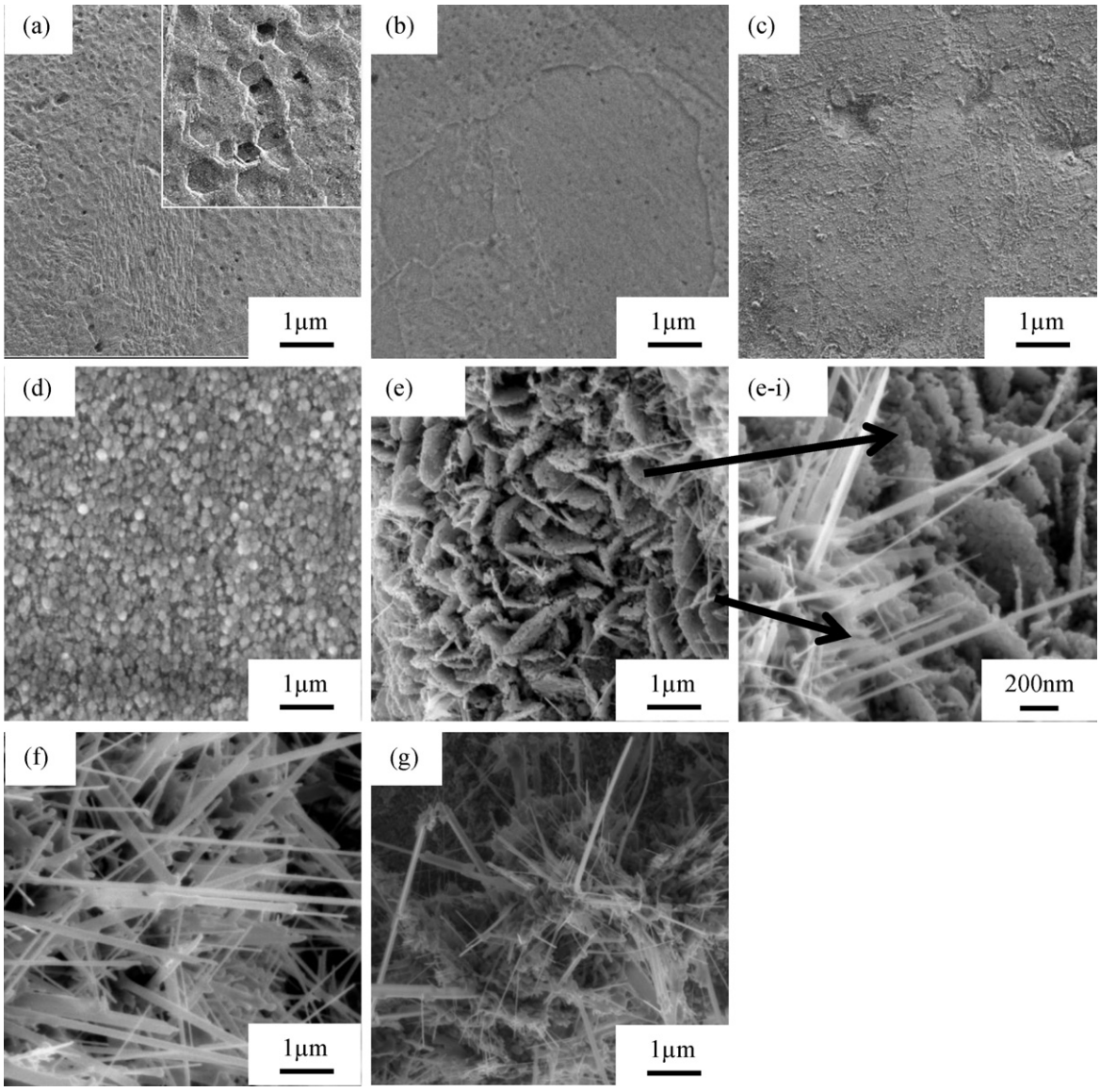

Fig. 1. Surface morphologies Zn foils, (a) before oxidation (after polishing and etching) and after oxidation at, (b) 100 °C, (c) 200 °C, (d) 300 °C, (e) 400 °C (low magnification), (e-i) 400 °C (high magnification), (f) 450 °C and (g) 500 °C. All oxidation processes were done in air for 30 min.

the phase investigation and photoluminescence spectroscopy was performed using a Jobin Yvon HR 800 UV.

3. Results and discussion

3.1. Structural and morphological properties

Surface morphology of the Zn foil after being etched in 5% HCl, is shown in Fig. 1(a). Inset in this figure is the higher magnification image of the etched surface. After oxidation, the surface of the foil changed dramatically depending on the oxidation temperatures. Fig. 1(b)–(g) is the FESEM images of the oxidised Zn foil at 100 °C, 200 °C, 300 °C, 400 °C, 450 °C and 500 °C, respectively. All samples were oxidised for 30 min in air. After oxidation at 100 °C, it could be seen that the surface of the foil is covered with thin oxide with preferential growth along the grain boundaries. As the oxidation temperatures were increased from 200 °C to 300 °C, the surface morphologies evolved from sparsely distributed spherical grains with diameters ranges from 30 to 50 nm (Fig. 1(c)) to a more dense structure (Fig. 1(d)). Oxidation at 400 °C produced surface oxide with a porous, flaky structure (Fig. 1(e)). Arrows pointing from Fig. 1(e) are showing the detailed morphologies at two spots: (i) the porous, flaky structure resembling nanosheets and (ii) nanorods that are seen emerging from the edge of the nanosheets. The nanosheets have a thickness averaged at ~50 nm and they are made out of particles with a diameter of ~30 nm. These particles are not bonded together, forming the open, porous structure. Nanorods that emerged from the edge of the nanosheets have a diameter of <10 nm and length reaching 1 μm.

As the oxidation temperature was increased to 450 °C, the length of the nanorods had increased to ~2 μm as seen in Fig. 1(f). At parts of the sample, the length of the nanorods could reach 5 μm. Moreover, a belt-like structure with submicron width is also detected. The belt-like structure becomes more prominent as the oxidation temperature was increased to 500 °C (Fig. 1(g)). Branches appear from the belt-like structure resembling dendrites.

Oxidation at a longer time of 1 h was then carried out to further investigate the morphologies of the oxidized Zn. Fig. 2(a)–(e) is the surface morphologies of Zn foil oxidised at 300 °C, 350 °C, 400 °C, 450 °C and 500 °C, respectively. Images shown on the left hand column marked with an 'i' are the low magnification images whereas images on the right hand column marked with an 'ii' are

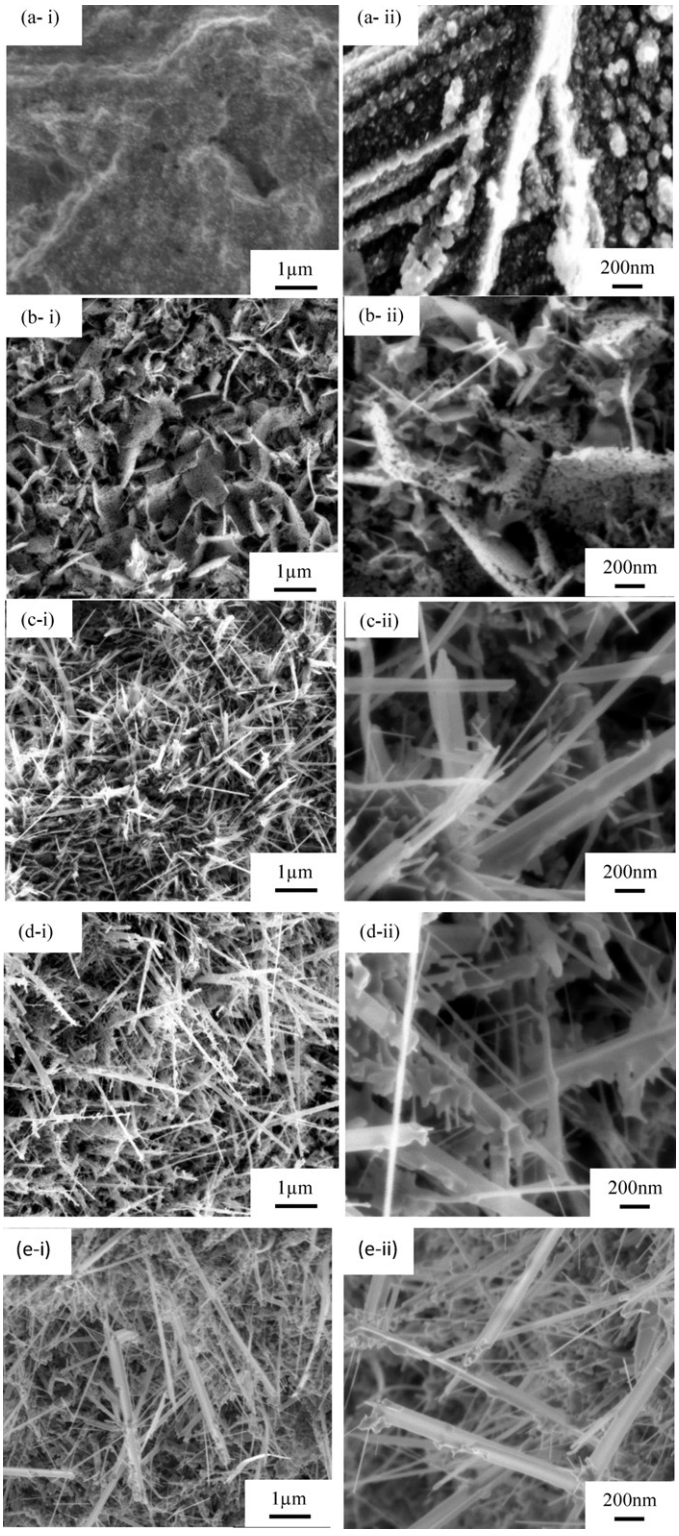

Fig. 2. Surface morphologies of the metallic Zn after being oxidized for 1 h at (a) 300 °C, (b) 350 °C, (c) 400 °C, (d) 450 °C and (e) 500 °C in air.

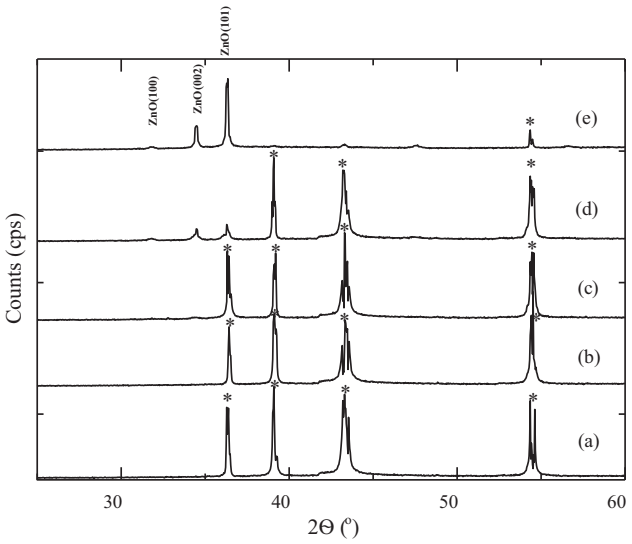

Fig. 3. XRD patterns of zinc oxidized at (a) 100 °C, (b) 200 °C, (c) 300 °C, (d) 350 °C and (e) 400 °C for 1 h in air.

the higher magnification images of the same samples. Oxidation for 1 h at 300 °C resulted in surface oxide with spherical, particulate-like grains as seen in Fig. 2(a-i and ii). Preferential growth occurs along the metal grain boundaries as well as along scratches induced by etching. The sample oxidised at 350 °C (Fig. 2(b-i)) has morphology similar to samples oxidised at 400 °C for 30 min. The oxide is consisted of porous nanosheets. From the higher magnification image (Fig. 2(b-ii)), nanorods are also seen emerging from the edge of the nanosheets. The sample oxidised for 1 h at 400 °C consists of branched rods covering the whole area of the foil, as seen in Fig. 2(c-i). In Fig. 2(c-ii), it can be seen that these rods have a diameter distribution from 10 nm to several microns with a length averaged at 2 μm. A belt-like structure with sub-micron width can also be detected and the structure becomes much obvious in the sample oxidised at 450 °C, as seen in Fig. 2(d-i and ii). Sub-micron rods formed in this sample also have branches with a diameter much smaller (in the range of 10–20 nm) than the main rod. The average length of the rods is 2 μm and at parts of the sample the length of the rods reaches more than 5 μm. Similar structures are observed in the sample oxidised at 500 °C for 1 h (Fig. 2(e-i)): sub-micron rods, nanorods and nanobelts. However, as seen in the higher magnification image in Fig. 2(e-ii), most of the rods have blunt tips and smaller diameter nanorods are seen to branch out from the rods.

Fig. 3 is the X-ray diffraction patterns for samples oxidised for 1 h at: (a) 100 °C, (b) 200 °C, (c) 300 °C and (d) 400 °C. From the patterns, only Zn peaks can be detected for samples oxidised at 100 °C and 200 °C (ICCD no. 00-004-0831). ZnO formed at very low temperature are expected to be very thin and amorphous; therefore, the diffraction peaks from the ZnO are expected to be rather broad with very small intensity. Higher intensity peaks can be detected for samples oxidised at 300 °C and 400 °C (Fig. 3(c) and (d)). The peaks are located at 2θ of 32.0°, 34.5°, and 36.5° corresponding to (1 0 0), (0 0 2) and (1 0 1) ZnO, respectively (ICDD no. 00-036-1451).

3.2. Luminescence properties

Fig. 4 shows the photoluminescence (PL) spectra for zinc foils oxidised at: (a) 100 °C, (b) 200 °C, (c) 300 °C and (d) 400 °C. As seen, no peaks can be seen for zinc oxidised at 100 and 200 °C (Fig. 4(a) and (b)). For samples oxidised at 300 and 400 °C the PL spectra have two prominent peaks: near band edge UV emission and the green emission (Fig. 4(c) and (d)). The UV emission at 380 nm is related to the emission from the recombination of electrons from the conduction band to the valance band (free excitonic emission). On the other hand, the green emission at 500 nm is related to defect states, in particular oxygen vacancies [12]. Sample oxidised at 300 °C is consisted of a rather flat thin oxide film as seen in Fig. 2(a), therefore the sample has the least defects. On the other hand, as seen in Fig. 2(d) sample oxidised at 400 °C is consisted of branched

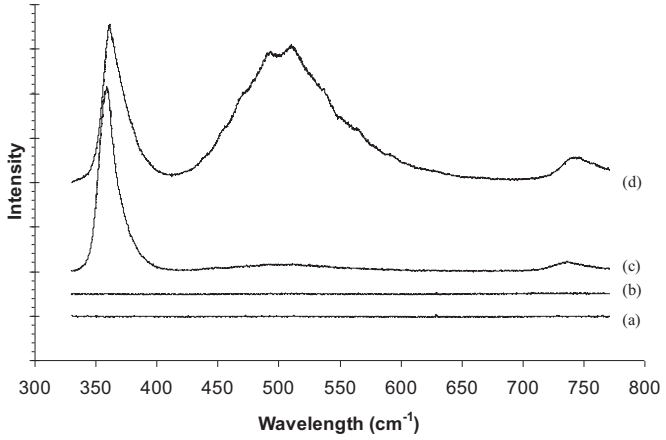

Fig. 4. Photoluminescence (PL) spectra for samples oxidised at: (a) 100 °C, (b) 200 °C, (c) 300 °C and (e) 400 °C for 1 h.

nanorods and sub-micron belts and hence defects at the boundaries are much higher explaining the green emission peak. Apart from oxygen vacancies, an excess of Zn may also account for the green emission. At this high temperature, more Zn ions will diffuse from the Zn foil, hence creating oxide with excess Zn. This would give rise to the green emission as well.

3.3. Growth mechanisms of ZnO nanostructures formed by thermal oxidation

Fig. 5 shows an evolution summary of the morphology of the ZnO as a function of oxidation temperature. Zinc is a metallic element with a low melting point of 419.6 °C [13]. Etched bare Zn is sketched in Fig. 5(a) and upon the exposure to the low oxidation temperature a passivated layer (initial oxide) will form rapidly on its surface. According to Cabrera and Mott, at this low temperature, adsorptions of oxygen on the surface of the native oxide will create strong field across the oxide (from the oxide|metal interface to the oxide|air interface). Due to the establishment of the field, Zn ions can be pulled through the oxide film outwards allowing growth of the ZnO [14]. However, the migration of Zn ions is thickness dependent, whereby the process will stop when the thickness of the ZnO reached around 10 nm. Growth can only be possible when Zn ions have extra energy to migrate to the oxide|air interface forming ZnO at this front. It has been accepted that the self-diffusion co-efficient of Zn ions in ZnO is much larger than oxygen ions at lower temperature regimes [15,16]. Assuming that the diffusion mechanism is via a vacancy mechanism, Nakamura et al. has suggested that a temperature of 150 °C is far too low for the Zn ions to diffuse through the initial oxidation layer [17]. However, growth at the grain boundaries may have been possible at the low temperature regimes due to the availability of the easy diffusion path along the grain boundaries (Fig. 5(b)). This is seen from the surface morphology of the oxidised Zn at 100 °C (Fig. 1(b)). At slightly higher temperatures, the migration of the Zn is possible. The formation of the oxides on the grains as well as at the grain boundaries can be seen in a sample oxidised at 200 °C (Fig. 1(c)). Upon closer inspection, the oxide appears to be in the form of spherical grains and the oxides are not being distributed evenly on the surface.

Oxidation at 300 °C for 30 min induced the formation of more of these spherical grains. At this point, the preferential growth at the grain boundaries is no longer prominent and the size of grains evidently became larger (Fig. 1(d)). The distribution of the grains is much more uniform and the surface of the oxide is relatively flat, as sketched in Fig. 5(c). The surface morphology does not change very much even after 1 h of oxidation. The flat oxide layer has a PL spectrum consisting of mainly that UV emission. This is related to perfect and stoichiometric ZnO crystals with minimum defects.

The formation of porous nanosheets can be as seen in Fig. 1(e) for a sample oxidised at 400 °C for 30 min and Fig. 2(b) for sample oxidised at 350 °C for 1 h. Upon closer inspection of the nanosheets, it could be seen that the sheets consist of weakly bonded, spherical ZnO crystals. The formation of these porous nanosheets can be explained by a vapour solid (VS) mechanism. As seen in the inset of Fig. 1(a), the surface of the Zn after being etched consists of hexagonal-shaped holes that correspond to (0 0 0 1) Zn grains. The (0 0 0 1) oriented grains do not oxidise very fast in comparison to sidewalls of the hexagonal Zn [18,19]. According to Gui et al. [20], in an oxidation of pure Zn nanoparticles, the surface of the particles are thought to be very loose and there is a Zn vapour aero-sphere hanging over the particles when the particles are heated. As the (0 0 0 1) face of Zn grains has a slower rate of oxidation, it is speculated that there is a tendency of the formation of this Zn vapour aero-sphere at the vicinity of the surface as shown in Fig. 5(d). Temperatures of 350 °C and 400 °C are high enough to allow a certain degree of sublimation of Zn, forming the Zn vapour as Zn melts at 419 °C. The vapour would, however, react quickly with oxygen forming ZnO nuclei. As the ZnO nuclei concentration increases and reaches supersaturation, growth occurs and the particles will be redeposited back onto the surface of the substrate to form the open, porous nanosheets (Fig. 5(e)). Such morphology has an extremely broad XRD pattern, indicative of the size of the nanocrystals. As the open, porous structure may have a large surface area, the corresponding defects existing at the surface may have been reflected by the existence of the green emission from the photoluminescence data of such sample. It is inferred that the etching process of the Zn foil, which was done to reveal the (0 0 0 1) Zn grains, may have contributed into the formation of this morphology. To date, no works on the formation of porous nanosheet by oxidation of Zn has been reported via VS mechanism.

The surface oxide of samples oxidised at 400 °C for 30 min and 350 °C for 1 h consist of nanorods protruding at the edge of the nanosheets. Increasing the oxidation temperature above 400 °C produced more nanorods, covering the surface of the metal more uniformly. As mentioned, at higher temperatures, diffusion of Zn ions will be much faster. Assuming that the diffusion is occurring only in a certain direction, favouring the migration of the Zn ions within the inner part of the rods, the growth would then occur at the tip of the oxide outwards, forming the rod-like structure. A similar observation was made by Li and Gao [16] on the oxidation of Zn in wet air. Since the diffusion process is thickness dependent, as the rods become longer the amount of Zn that could diffuse to the tip becomes lesser causing the sharp-ended tip. The morphology is termed nanoneedles by several authors including Umar et al. [8] and Yu et al. [5] and is sketched in Fig. 5(f).

The sample oxidised at 450 °C resulted in the formation much more uniform ZnO nanorods but with blunt tips. As stated previously, the formation of the nanorods occurs by fast diffusion of Zn ions via a particular diffusion channel inside the rods towards the tip of the nanorods. Therefore, at the tip of the nanorods, Zn ions will accumulate and as the oxidation temperature is above the meting point of Zn, the accumulated Zn at the tip of the rods will melt, forming blunt tips as seen in Fig. 2(d-ii).

Oxidation at temperatures above 500 °C has resulted in the formation of branched nanorods as seen in Figs. 1(g) and 2(e) for samples oxidised at 30 min and 1 h, respectively. According to the Gibbs–Thomson effect, as discussed by Hejazi et al., the growth rates of the ZnO nanorods are inversely proportional to the radius of the nanorods formed [21]. This indicates that the growth rate decreases with increasing nanorod diameter. The increase of the nanorod diameter can also originate from the migration of material from one rod to the other, as illustrated in Fig. 5(g). This results

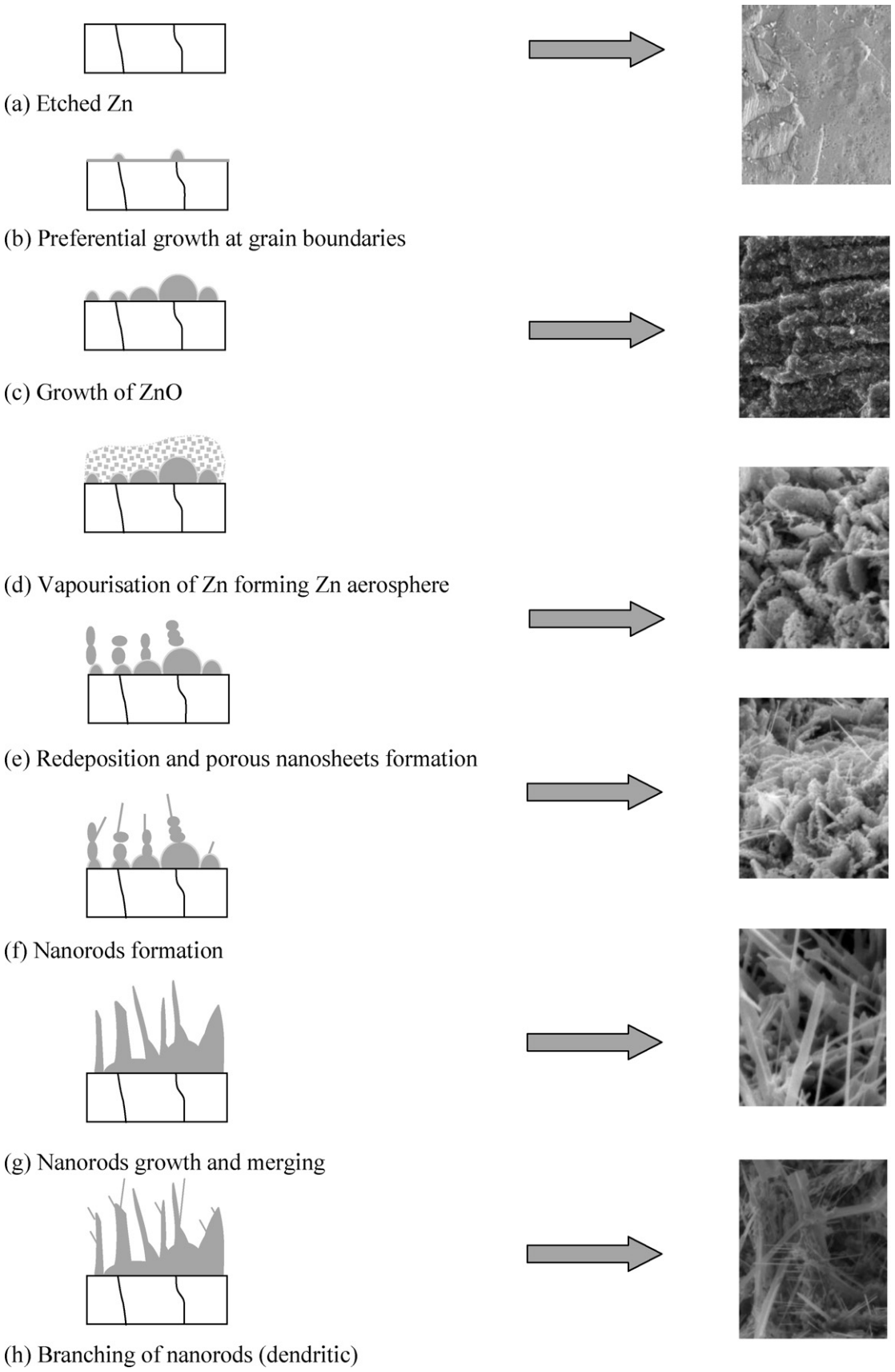

Fig. 5. Schematic illustration of growth of ZnO nanowires and nanosheets on the surface of etched Zn foil by oxidation in air.

in a merging of smaller rods forming sub-micron rods and belt-like structure, as seen from the FESEM in Fig. 2(e). From this figure, it can also be seen that at the blunt tips where partial melting was thought to occur, smaller nanorods emerge forming the branched nanorods. At this temperature, secondary growth leads to the formation of dendritic nanorods. This is sketched in Fig. 5(h).

4. Conclusion

Oxidation of etched Zn resulted in the formation of ZnO nanostructures with morphology dependent on the oxidation temperatures and times. Oxidation at temperatures <300 °C resulted in a relatively flat oxide. At 350 °C, the oxide is in a form of open, porous nanosheets with thickness of 50 nm. The nanosheets were produced via oxidation of Zn vapour. At 400 °C, 2 μm ZnO nanorods formed and above the melting point of Zn, blunt nanorods were produced. At these temperatures, some of the nanorods merged to form a belt-like structure and the nanorods started to branch out forming a dendritic nanostructure. The length of the nanorods increased with the increase of temperature. The longest nanorods could reach 10 μm but the average length is 5 μm for the sample oxidised at 450 °C. The photoluminescence of ZnO is morphology dependent with much more green emission as the nanostructure becomes apparent. This indicates more oxygen vacancies and/or excess Zn in the nanostructure.

References

[1] U. Ozgur, Ya.I. Alivov, A. Teke, M.A. Reshchikov, S. Dogan, V. Avrutin, S.-J. Cho, H. Morkoc, A comprehensive review of ZnO materials and devices, J. Appl. Phys. 98 (2005) 1–103.
[2] J.-H. Sun, S.-Y. Dong, Y.-K. Wang, S.-P. Sun, Preparation and photocatalytic property of a novel dumbbell-shaped ZnO microcrystal photocatalyst, J. Hazard. Mater. 172 (2009) 1520–1526.
[3] N. Kaneva, I. Stambolova, V. Blaskov, Y. Dimitriev, S. Vassilev, C. Duskin, Photocatalytic activity of nanostructured ZnO films prepared by two different methods for the photoinitiated decolorization of malachite green, J. Alloys Compd. 500 (2010) 252–258.
[4] S.L. Wang, X. Jia, P. Jiang, H. Fang, W.H. Tang, Large-scale preparation of chestnut-like ZnO and Zn–ZnO hollow nanostructures by chemical vapor deposition, J. Alloys Compd. 502 (2010) 118–122.
[5] W. Yu, C. Pan, Low temperature thermal oxidation synthesis of ZnO nanoneedles and the growth mechanism, Mater. Chem. Phys. 115 (2009) 74–79.
[6] S.J. Chen, J.G. Ma, D.X. Zhao, Z.Z. Zhi, Y.M. Lu, J.Y. Zhang, D.Z. Shen, X.W. Fan, High quality ZnO thin films prepared by two-step thermal oxidation of metallic Zn, J. Cryst. Growth 240 (2002) 467–472.
[7] Y.I. Alivov, A.V. Chernykh, M.V. Chukichev, R.Y. Korotkov, Thin polycrystalline zinc oxide films obtained by oxidation of metallic zinc films, Thin Solid Films 473 (2005) 241–246.
[8] A. Umar, S.H. Kim, Y.-S. Lee, K.S. Nahm, Y.B. Hahn, Catalyst-free large-quantity synthesis of ZnO nanorods by vapour–solid growth mechanism: structural and optical properties, J. Cryst. Growth 282 (2005) 131–136.
[9] C.L. Xu, D.H. Qin, H. Li, Y. Guo, T. Xu, H.-L. Li, Low-temperature growth and optical properties of radial ZnO nanowires, Mater. Lett. 58 (2004) 3976–3979.
[10] M.S. Aida, E. Tomasella, J. Cellier, M. Jacquet, N. Bouhssira, S. Abed, A. Mosbah, Annealing and oxidation mechanism of evaporated zinc thin films from zinc oxide powder, Thin Solid Films 515 (2006) 1494–1499.
[11] Y. Ma, G.T. Du, S.R. Yang, Z.T. Li, B.J. Zhao, X.T. Yang, T.P. Yang, Y.T. Zhang, D.L. Liu, Control of conductivity type in undoped ZnO thin films grown by metalorganic vapour phase epitaxy, J. Appl. Phys. 95 (11) (2004).
[12] J. Zhao, L. Hu, Z. Wang, Y. Zhao, X. Liang, M. Wang, High-quality ZnO thin films prepared by low temperature oxidation of metallic Zn, Appl. Surf. Sci. 229 (2004) 311–315.
[13] J.F. Garcia, S. Sanchez, R. Metz, Complete oxidation of zinc powder. Validation of kinetics models, Oxid. Met. 69 (2008) 317–325.
[14] N. Cabrera, N.F. Mott, Theory of the oxidation of metals, Rep. Prog. Phys. 12 (1948–1949) 163.
[15] S.R. Hejazi, H.R. Madaah Hosseini, M. Sasani Ghamsari, The role of reactants and droplet interfaces on nucleation and growth of ZnO nanorods synthesized by vapour–solid–liquid (VLS) mechanism, J. Alloys Compd. 455 (2008) 353–357.
[16] Z.W. Li, W. Gao, Growth of zinc oxide thin films and nanostructures by wet oxidation, Thin Solid Films 515 (2007) 3323–3329.
[17] R. Nakamura, J.-G. Lee, D. Tokozakura, H. Mori, H. Nakajima, Formation of hollow ZnO through low temperature oxidation of Zn nanoparticles, Mater. Lett. 61 (2007) 1060–1063.
[18] H.J. Fan, R. Scholz, F.M. Kolb, M. Zacharias, Two-dimensional dendritic ZnO nanowires from oxidation of Zn microcrystals, Appl. Phys. Lett. 85 (18) (2004).
[19] C.X. Xu, X.W. Sun, Zinc oxide nanodisk, Appl. Phys. Lett. 85 (17) (2004).
[20] Y. Gui, C. Xie, Q. Zhang, M. Hu, J. Yu, Z. Weng, Synthesis and characterization of ZnO nanostructures by two-step oxidation of Zn nano- and microparticles, J. Cryst. Growth 289 (2006) 663–669.
[21] S.R. Hejazi, H.R. Maadah, M. Hosseini, A diffusion-controlled kinetic model for growth of Au-catalyzed ZnO nanorods: theory and experiment, J. Cryst. Growth 309 (2007) 70–75.